Molecular BioSystems

Accepted Manuscript

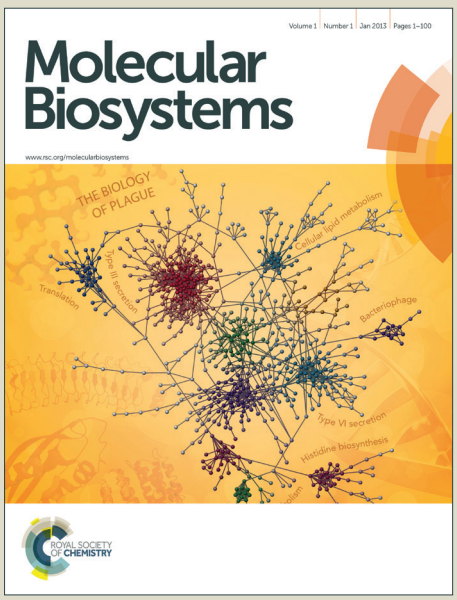

ROYAL SOCIETY OF CHEMISTRY

www.rsc.org/molecularbiosystems

Molecular BioSystems

PAPER

A metal carbonyl-protein needle composite designed for intracellular CO delivery to modulate NF-κB activity†

Received 00th January 20xx,
Accepted 00th January 20xx

DOI: 10.1039/x0xx00000x

www.rsc.org/

Hiroshi Inaba,[a] Nusrat J. M. Sanghamitra,[b] Kenta Fujita,[c] Takeya Sho,[c] Takahiro Kuchimaru,[c] Susumu Kitagawa,*[a,b] Shinae Kizaka-Kondoh[c] and Takafumi Ueno*[b,c]

Carbon monoxide (CO) has been recognized as a messenger for signal transduction in living cells and tissues. For intracellular CO delivery, several metal carbonyl complexes have been used as CO-releasing molecules (CO-RMs). To improve the properties of CO-RMs, such as the stability and the CO release rate, ligands and carriers of the metal complexes have been exploited. Here we report the development of an efficient intracellular CO delivery system using a protein scaffold. We used a protein needle reconstructed from gene product 5 of bacteriophage T4, which has high cellular permeability and stability. When ruthenium carbonyl complexes are conjugated to the needle using a His-tag triad at the C-terminus, the resulting composite has a signicantly higher cellular uptake efficiency of Ru carbonyl and a 12-fold prolonged CO release rate relative to $Ru(CO)_3Cl$(glycinate), a widely used CO-RM. We demonstrate that CO delivered by the composite activates the transcriptional factor nuclear factor-kappaB (NF-κB), which in turn, leads to significant induction of expression of its target genes, *HO1*, *NQO1*, and *IL6* through generation of reactive oxygen species (ROS). The signaling pathway is distinct from that of tumor necrosis factor (TNF)-α-induced activation of NF-κB. The protein needle-based CO-RM can be exploited to elucidate biological functions of CO and used in the development of protein-based organometallic tools for modulation of cellular signaling.

Introduction

Carbon monoxide (CO) serves as a versatile signaling molecule in anti-inflammatory, anti-proliferative, and anti-apoptotic cellular processes.[1-4] Since the localization and levels of CO are critical in these signaling processes, metal carbonyl complexes known as CO-releasing molecules (CO-RMs) have been developed to deliver CO into living cells in a safe fashion.[1,2,5-9] Examples of such CO-RMs include $[Ru(CO)_3Cl_2]_2$ (CORM-2) and $Ru(CO)_3Cl$(glycinate) (CORM-3). CO-RMs with various ligands have been synthesized to modulate their CO-releasing properties.[1] To improve the stability and pharmacokinetic properties of CO-RMs, incorporation of CO-RMs into macromolecular carriers such as proteins, micelles, nanoparticles, and dendrimers has been exploited.[5,10-17] However, the low cellular permeability and low stability of the carrier molecules remain problematic. A carrier that can stabilize CO-RMs and improve their cellular uptake is required to advance our understanding of intracellular CO signaling mechanisms.

Proteins are promising CO-RM carriers because they can stabilize the coordination structures of organometallic compounds in a cellular environment.[5] Although protein-$Ru(CO)_2$ composites have been reported,[10-12] these composites have poor cellular uptake efficiency. Proteins with high cell permeability will be useful for more efficient CO delivery. Thus, we used a β-helical protein needle (β-PN) to address this requirement.[18] β-PN is a robust molecular needle reconstructed from the triple-stranded β-helix motif of gene product 5, a cell membrane-puncturing protein 5 of bacteriophage T4 (Fig. 1a).[18] We have reported that β-PN efficiently penetrates living cells via an endocytosis-independent pathway.[19] During the uptake process, the needle structure is maintained without decomposition or aggregation. The β-PN's cell-penetrating activity has been utilized for intracellular delivery of the exogenous proteins.[20] The results prompted us to investigate this robust cell-penetrating protein needle as a carrier for CO-RMs.

Here we report the development of an efficient CO delivery system using β-PN to elucidate signaling of intracellular CO which is involved in activation of nuclear factor-kappaB (NF-κB), a transcriptional factor (Fig. 1b). NF-κB, which is a key transcriptional regulator of a variety of genes including pro-inflammatory and antiapoptoticgenes, is considered one of the therapeutic targets of CO.[21] CO gas, CORM-2 and CORM-3

[a] Department of Synthetic Chemistry and Biological Chemistry, Graduate School of Engineering, Kyoto University, Katsura, Nishikyo-ku, Kyoto 615-8510, Japan.
[b] Institute for Integrated Cell-Material Sciences (WPI-iCeMS), Kyoto University, Yoshida, Sakyo-ku, Kyoto 606-8501, Japan. E-mail: kitagawa@icems.kyoto-u.ac.jp
[c] Department of Biomolecular Engineering, Graduate School of Bioscience and Biotechnology, Tokyo Institute of Technology, Nagatsuta-cho, Midori-ku, Yokohama 226-8501, Japan. E-mail: tueno@bio.titech.ac.jp
† Electronic Supplementary Information (ESI) available: See
DOI: 10.1039/x0xx00000x

show the cytoprotective effects by modulating NF-κB activity and subsequent gene expression.[22-31] Although activation of NF-κB under normal physiological conditions is also important signaling pathways involving CO, as indicated by investigations using CO gas,[22,23] the effect of intracellularly-delivered CO has not been elucidated using the previously employed CO-RMs. We constructed a CO-releasing protein needle with the aim of evaluating intracellular signaling of CO involving activation of NF-κB. The CO-releasing protein needle was constructed by conjugation of $Ru(CO)_2$ fragments to a hexahistidine fragment (His-tag) at the C-terminus (**β-PN_Ru**). **β-PN_Ru** has a significantly higher cellular uptake efficiency of Ru carbonyl and a 12-fold prolonged CO release rate compared to CORM-3. The intracellular CO delivered by **β-PN_Ru** activates NF-κB by generation of reactive oxygen species (ROS) under conditions where CORM-3 has no effect. The activation of NF-κB significantly leads to expression of its target genes *HO1*, *NQO1* and *IL6*. The gene expression is not induced by tumor necrosis factor (TNF)-α which activates NF-κB by a ROS-independent pathway. Thus, we demonstrate that intracellular CO is responsible for the efficient therapeutic response through modulation of the ROS-mediated NF-κB activation. The Ru carbonyl-protein needle composite can serve as an efficient and convenient CO delivery system for elucidation of CO functions and it is expected to also be useful for therapeutic applications.

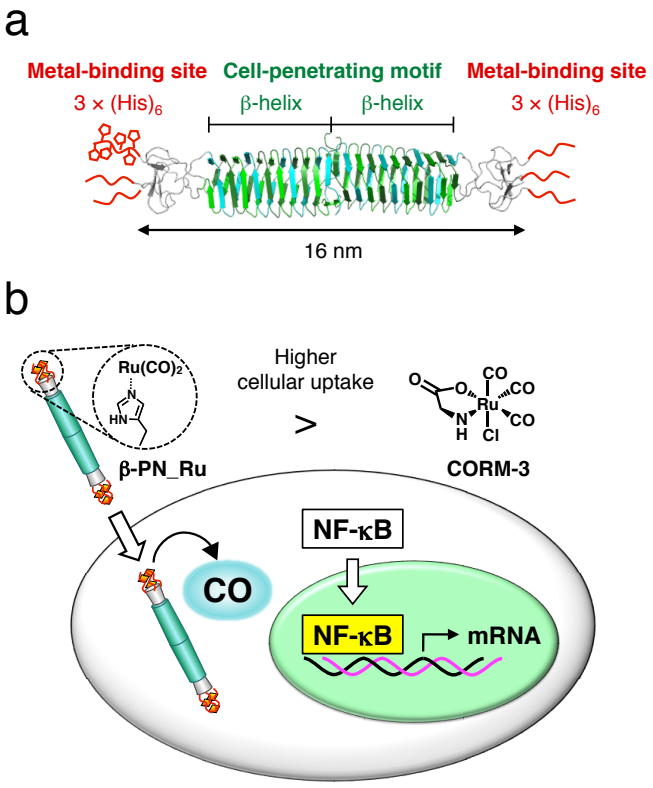

Fig. 1 A Ru carbonyl-protein needle composite for modulation of activation of nuclear factor-kappaB (NF-κB). (a) Structure of the β-helical protein needle (β-PN) derived from X-ray crystallography.[18] The β-helical domain and the triads of His-tags at the C-termini are shown in green and red, respectively. (b) Schematic drawing of penetration of the Ru carbonyl protein needle (**β-PN_Ru**) into the cell and activation of NF-κB. **β-PN_Ru** is internalized into cells with a significantly higher efficiency than CORM-3 and releases CO to activate NF-κB, resulting in the expression of the target mRNAs.

Results and discussion

Design and synthesis of the Ru carbonyl-protein needle composite

To incorporate $Ru(CO)_2$ moieties into β-PN, triads of His-tags, each including six histidines at the both end of β-PN were used (Fig. 1a). It has been reported that a reaction between a His residue of lysozyme and CORM-3 results in introduction of a $Ru(CO)_2$ moiety into lysozyme.[11] The presently designed system has a triad of His-tags in order to obtain even more stable ligation to Ru carbonyls in order to retain Ru coordination on β-PN after release of CO.[32] The β-PN with $Ru(CO)_2$ (**β-PN_Ru**) was prepared by reaction of the His-tags of β-PN with CORM-2 (Fig. 2a). Ru carbonyls are expected to coordinate the His-tag of β-PN selectively because β-PN is histidine-free except for the His-tag (see experimental section). A methanol solution of CORM-2 (6 equivalents) was added to β-PN (5.0 μM) in 20 mM Tris/HCl pH 8.0. After stirring for 3 h at 25°C, the mixture was purified with Sephadex G-25 equilibrated with 0.1 M sodium phosphate pH 7.0. As a negative control, an "inactivated," carbonyl-free β-PN Ru composite (**β-PN_iRu**) was synthesized by the same procedure as for **β-PN_Ru** except that $Ru(DMSO)_4Cl_2$ was used instead of CORM-2. The numbers of Ru atoms of **β-PN_Ru** and **β-PN_iRu**, determined by inductively coupled plasma mass spectroscopy (ICP-MS) and the bicinchoninic acid (BCA) protein assay, were found to be 6.4 and 6.0, respectively. The sizes of **β-PN_Ru** and **β-PN_iRu** determined by dynamic light scattering are 10.7 ± 1.9 and 9.1 ± 1.7 nm, respectively (Fig. S1). The values are similar to that of β-PN (10 nm),[19] showing that the needle structures were maintained after the modifications. The attenuated total reflectance (ATR)-IR spectrum of **β-PN_Ru** has two characteristic bands in the carbonyl vibration region at 2031 cm^{-1} and 1955 cm^{-1}, which originate from the previously reported *cis*-$Ru(CO)_2$ fragment (Fig. 2b, solid line).[11,33] **β-PN_iRu** has no specific peaks in this region (Fig. 2b, dashed line). The MALDI-TOF mass spectrum of the monomer of **β-PN_Ru** (14966 Da) indicates a mass increment of 164 Da compared to the monomer of β-PN (14802 Da), which is assigned to $Ru(CO)_2$ (calcd. 157 Da) (Fig. 2c). Since β-PN is formed by head-to-head dimerization of the trimer structures, the result indicates that three $Ru(CO)_2$ fragments are linked to the His-tags of the C-termini of β-PN. The mass increment was not observed after the reaction between β-PN with no His-tag [β-PN(ΔHis-tag)] and CORM-2 (Fig. S2). Thus, the *cis*-$Ru(CO)_2$ fragments were successfully introduced at both of the C-termini of β-PN with ligation to the triad of His-tags.

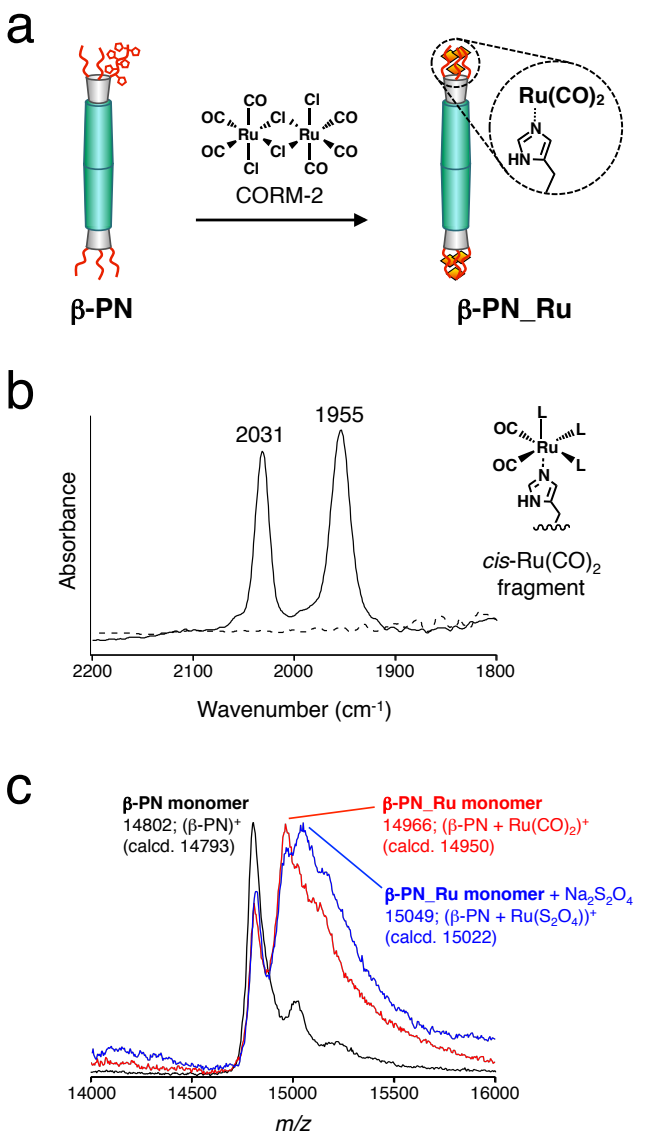

Fig. 2 Construction and characterization of **β-PN_Ru**. (a) Conjugation of the $Ru(CO)_2$ fragments to β-PN in a reaction of a His-tag and CORM-2 (construction of **β-PN_Ru**). (b) ATR-IR spectra of **β-PN_Ru** (solid line) and **β-PN_iRu** (dashed line) in 0.1 M sodium phosphate pH 7.0. The pair of CO stretching vibrations of **β-PN_Ru** is assigned to the *cis*-$Ru(CO)_2$ fragment (L = ligand). (c) MALDI-TOF mass spectra of the monomers of β-PN (black), **β-PN_Ru** (red), and **β-PN_Ru** after reaction with $Na_2S_2O_4$ (blue). In the reaction, **β-PN_Ru** (4.0 μM) was added to $Na_2S_2O_4$ (20 mM) in 0.1 M sodium phosphate pH 7.0 and the mixture was stirred at 25°C for 2 h.

CO release properties

The release of CO from **β-PN_Ru** was assessed by measuring the conversion of deoxymyoglobin (deoxy-Mb) to carbonmonoxy-myoglobin (MbCO) in 10 mM PBS in the presence of 6.9 mM $Na_2S_2O_4$ under an Ar atmosphere.[8] The amount of released CO per Ru carbonyl equivalent was plotted over time and was found to follow pseudo first order kinetics (Fig. S3a and S3b).[34] The total amount of released CO per Ru carbonyl (equivalent of CO) and half-life time ($t_{1/2}$) of release of CO from Ru carbonyl were calculated from the fitted curves. The total amount of released CO from **β-PN_Ru** is 0.16 ± 0.01 equiv per Ru carbonyl. The $t_{1/2}$ of CO release of **β-PN_Ru** is 26.2 ± 0.15 min, which is 12-fold longer relative to that of CORM-3 (2.2 min) evaluated under the similar conditions.[10] The slow release of CO suggests that the triad of his-tags provides stability to the *cis*-$Ru(CO)_2$ structure at both ends of **β-PN_Ru**. It has been indicated that $Na_2S_2O_4$, which is used in the Mb assay, is implicated in triggering CO release from CO-RMs.[5,13,35] To evaluate whether CO is released from the **β-PN_Ru** by reaction with $Na_2S_2O_4$, a MALDI-TOF measurement was carried out after addition of $Na_2S_2O_4$ to **β-PN_Ru**. A new peak was identified and assigned to the species formed by addition of a $Ru(S_2O_4)$ fragment to β-PN (Fig. 2c). This indicates that CO is released from **β-PN_Ru** by the reaction with $Na_2S_2O_4$ even in the absence of Mb. Endogenous thiol compounds such as glutathione and cysteine, which are abundant in cytoplasm at millimolar concentrations, are expected to trigger the intracellular CO release from CO-RMs.[13,36] The Mb assay was carried out in the presence of 5 mM glutathione and 150 mM KCl to mimic the intracellular environment (Table S1). The amount of released CO from **β-PN_Ru** and CORM-3 decreased under the condition. The result corresponds to the previous study showing that glutathione decreased the amount of released CO compared to $Na_2S_2O_4$.[13] Oxy-hemoglobin (oxy-Hb) was used to assess CO release from **β-PN_Ru** in the absence of $Na_2S_2O_4$.[35] After incubation of oxy-Hb with **β-PN_Ru** for 90 min, there was no significant change in spectrum of oxy-Hb, indicating that CO is not released from **β-PN_Ru** in the absence of $Na_2S_2O_4$ (Fig. S3c). These results suggest that **β-PN_Ru** will release CO after uptake into cells by reaction with endogenous glutathione and cysteine.

Cellular uptake analysis

Cellular uptake of **β-PN_Ru** was confirmed by confocal microscopy for **β-PN_Ru** modified with the green fluorescence dye ATTO520 (see supporting information). Green fluorescence was observed in HEK293 cells after incubation with the needle for 12 h, indicating that internalization of **β-PN_Ru** occurs even after modification of the $Ru(CO)_2$ moiety (Fig. S4). Intracellular CO release from **β-PN_Ru** was confirmed by using CO Probe 1 (COP-1), which selectively reacts with CO to produce a fluorescent product.[37] HEK293/κB-Fluc cells, which were established to monitor NF-κB activity by a luciferase reporter assay according to previously reported method,[38] were incubated with **β-PN_Ru** for 60 min. These cells were then treated with COP-1 for 30 min. As shown in Fig. 3a and 3b and quantified in Fig. 3c, an obvious increase in intracellular green fluorescence was observed in the **β-PN_Ru** treated cells. The results show that **β-PN_Ru** can release CO in the cells within 60 min. The cellular uptake efficiency of **β-PN_Ru** into HEK293/κB-Fluc cells was determined according to the previously reported method.[10,13] After incubation of the cells with **β-PN_Ru** for 24 h, the cells were collected and lysed. The concentration of Ru

atoms in the cell lysate was determined using ICP-MS. The uptake efficiency was calculated by comparing the amount of Ru atoms used in the assay and the amount of Ru atoms in the cell lysate (see Methods). The uptake efficiency value of Ru atoms of **β-PN_Ru** measured after 24 h was found to be 1.4%. In contrast, uptake of CORM-3 at the same Ru concentration for **β-PN_Ru** (10 μM) was not detected by ICP-MS. This suggests that **β-PN_Ru** delivers Ru carbonyl with significantly higher uptake efficiency than CORM-3. The uptake efficiency of **β-PN_Ru** is about 20-fold higher than that of the protein cage of ferritin (Fr) and $Ru(CO)_2$ composites (Fr-CO-RM composites).[10] The MTT assay was performed to assess cell viability after a 25 h period of incubation with **β-PN_Ru** (Fig. S5). The cell viability of HEK293/κB-Fluc cells in the presence of 10 and 20 μM Ru carbonyl of **β-PN_Ru** is not altered relative to that of untreated cells. These results indicate that **β-PN_Ru** and its byproduct after CO liberation are non-toxic to the cells. Thus, **β-PN_Ru** can conveniently deliver CO into living cells without cytotoxicity.

NF-κB activity

The effect of **β-PN_Ru** on NF-κB activity was assessed using HEK293/κB-Fluc cells, which express firefly luciferase in response to NF-κB activation.[10,38] We observed activation of NF-κB in HEK293/κB-Fluc cells upon addition of tumor necrosis factor (TNF-α) in a concentration- and time-dependent manner (Fig. S6). After pre-incubation of HEK293/κB-Fluc cells with **β-PN_Ru**, **β-PN_iRu** or CORM-3 for 1 h, the cells were additionally incubated for 24 h. The significant increase in bioluminescence intensity induced by **β-PN_Ru** indicates that CO released from **β-PN_Ru** activates NF-κB because carbonyl-free **β-PN_iRu** has no effect on NF-κB activity (Fig. 4a). It was found that CORM-3 and one of the Fr-CO-RM composites (RuCO•apo-E45C/C48A-rHLFr) have no significant effect on the NF-κB activation (Fig. 4a and S7).[10]

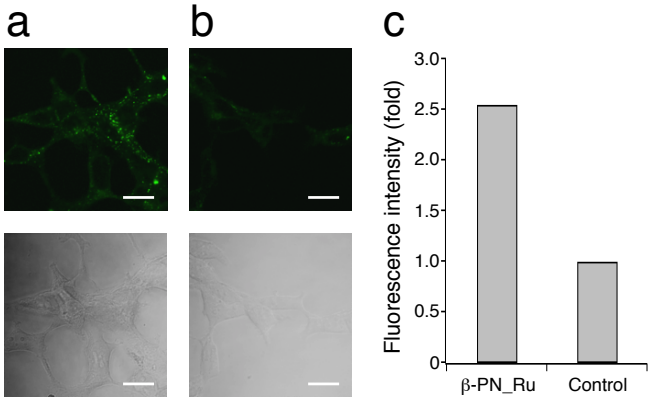

Fig. 3 Detection of intracellular CO using CO Probe 1 (COP-1). Confocal fluorescence (top) and bright field (bottom) images of HEK293/κB-Fluc cells incubated with (a) **β-PN_Ru** (40 μM Ru carbonyl) for 60 min, and then 1 μM COP-1 for 30 min, (b) 1 μM COP-1 for 30 min, at 37°C under 5% CO_2 (Control) (scale bars, 20 μm). (c) Quantification of fluorescence intensity per cell area.

Thus, **β-PN_Ru** can activate NF-κB as a result of the cooperative effects provided by high cell permeability and sustained CO release. Fig. 4b shows the bioluminescence intensities measured after 12- and 24-h incubation periods upon addition of **β-PN_Ru** (1, 10, and 20 μM). **β-PN_Ru** activates NF-κB in a concentration-dependent manner during the incubation periods, showing that a specific level of intracellular CO is critical to initiate activation of NF-κB.

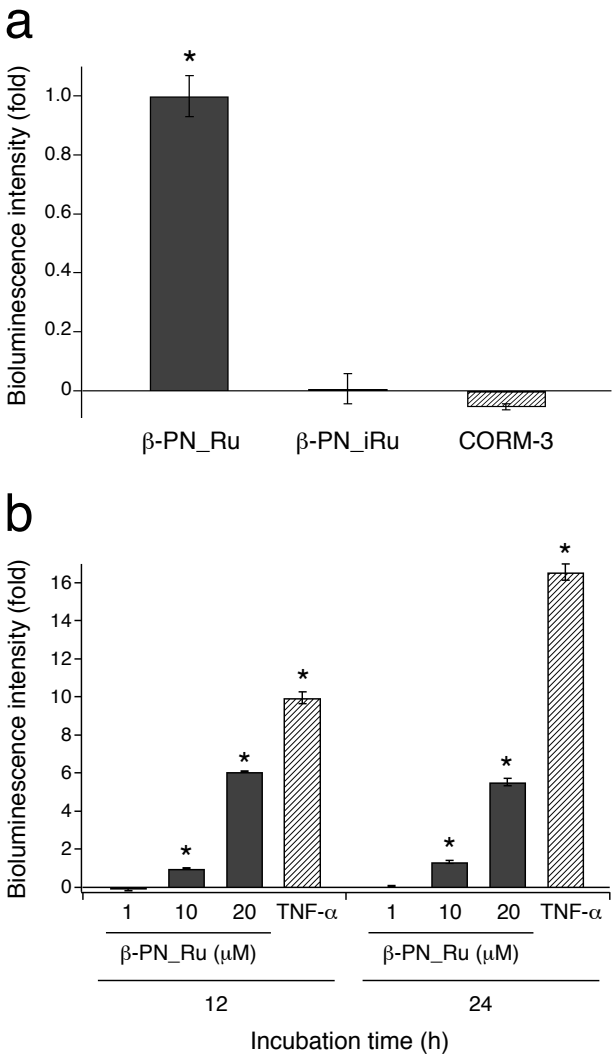

Fig. 4 Effect of CO release of **β-PN_Ru** on NF-κB activity. (a) Effect of **β-PN_Ru**, **β-PN_iRu**, and CORM-3 (10 μM Ru ions) on NF-κB activity after a 24 h incubation period. (b) Concentration dependence of **β-PN_Ru** (1, 10, and 20 μM Ru carbonyl) on NF-κB activity. TNF-α (0.3 ng/mL) was used as a positive control. In each experiment, HEK293/κB-Fluc cells were pre-incubated with **β-PN_Ru**, **β-PN_iRu**, or CORM-3 for 1 h. Subsequently, the cells were cultured for 12 and 24 h. The NF-κB activity was assessed by monitoring changes in the bioluminescence intensity as a result of luciferase activity. The data show the subtracted bioluminescence intensity of the cells that were treated with each sample from that of the negative control cells treated with buffer (0.1 M sodium phosphate pH 7.0). *P < 0.05 compared to the negative control cells

at each incubation time point. Each experiment was performed three times and the data represent mean ± SEM.

Signaling pathways

A high affinity of CO for different cellular heme proteins results in up-regulation or down-regulation of levels of ROS.[4,39] The generation of low-levels of ROS by CO is important and tightly regulated to trigger adaptive responses and cell survival by activation of transcriptional factors and protein kinases.[39] Accordingly, the effect of **β-PN_Ru** on generation of ROS in HEK293/κB-Fluc cells was evaluated using the luminescence-based ROS-detecting assay kit. **β-PN_Ru** induces generation of ROS after 6-h to 12-h incubation periods while CORM-3 has no effect (Fig. 5a). This indicates that intracellular CO delivered by **β-PN_Ru** increases the level of ROS to activate NF-κB. TNF-α was found to have less of an effect on generation of ROS (Fig. 5a) although it can activate NF-κB (Fig. S6). Thus, TNF-α induces a different signaling pathway than **β-PN_Ru** in the activation of NF-κB. The generation of ROS was found to be inhibited by **β-PN_Ru** after a 24-h incubation period (Fig. 5a), indicating that a feedback pathway is involved in regulating the amount of ROS. Quantitative reverse transcription PCR (qRT)-PCR was performed to examine whether **β-PN_Ru** influences mRNA expression of a NF-κB target gene. HO-1 is expressed by stimuli including oxidative stress and provides anti-oxidant and anti-inflammatory effects via inhibition of NF-κB activation by decreasing the amount of ROS.[25,40] NAD(P)H:quinone oxidoreductase 1 (NQO1), which can be induced by CO and oxidative stress,[41] is implicated in detoxification of ROS involved in the NF-κB activation pathway.[42,43] Interleukin-6 (IL-6) is a typical inflammatory cytokine that is regulated via the action of NF-κB.[44] The expression level of the mRNA was found to be significantly increased by **β-PN_Ru** at 12 h whereas **β-PN_iRu**, CORM-3 and TNF-α show less of an effect (Fig. 5b). The activation of these genes by **β-PN_Ru** was not observed at 24 h (Fig. 5b). The result is consistent with the decreased amount of ROS by **β-PN_Ru** at 24 h (Fig. 5a). Thus, the ROS-mediated activation of NF-κB by **β-PN_Ru** can efficiently induce gene expression in a manner distinct from that of TNF-α in activation of NF-κB. The pathway of TNF-α-induced NF-κB activation shows less of an effect on generation of ROS and gene expression (Fig. 5).

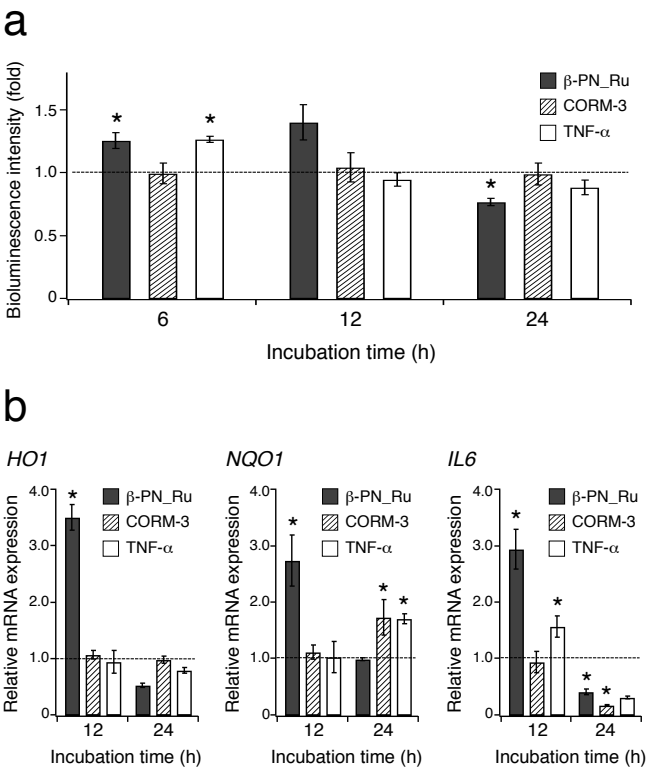

Fig. 5 Effect of **β-PN_Ru** and CORM-3 on signaling related to NF-κB activation. (a) Generation of ROS. (b) Expression of mRNA. In each experiment, HEK293/κB-Fluc cells were pre-incubated with **β-PN_Ru** or CORM-3 (10 μM Ru carbonyl) for 1 h. TNF-α (1.0 ng/mL) was used for comparison. Subsequently the cells were cultured for 6, 12, and 24 h. The amount of ROS was determined by ROS-Glo assay (Promega). Expressions levels of *HO1*, *NQO1*, and *IL6* were determined by qRT-PCR. The expression of each gene was normalized to the level of β-actin mRNA. The relative bioluminescence intensity in ROS-Glo assay and the relative mRNA expression level of each gene were normalized at each time period by using the negative control cells which were treated with buffer (0.1 M sodium phosphate pH 7.0, normalized to 1.0). **P* < 0.05 compared to the negative control cells. Each experiment was performed three times and the data represent mean ± SEM.

Discussion

Efficient CO delivery can be accomplished by coordination of $Ru(CO)_2$ to β-PN. β-PN retains the $Ru(CO)_2$ moiety by selectively binding to His-tag triads at the C-termini (Fig. 1a and 2a). The coordination of the His-tag to the Ru carbonyls can be accomplished while maintaining the *cis*-$Ru(CO)_2$ structure which provides sustained CO release as shown previously.[10] The longer $t_{1/2}$ value (26.2 min) of **β-PN_Ru** relative to that of CORM-3 (2.2 min) is advantageous for CO delivery to the intracellular targets. The chelation of the $Ru(CO)_2$ moiety by the His-tag triads effectively holds CO in place and prevents ligand exchange with glutathione or cysteine.[32,36] **β-PN_Ru** has a higher uptake efficiency of Ru carbonyl compared to CORM-3. The uptake efficiency of Ru carbonyl of **β-PN_Ru** is expected to be significantly higher than that of a CO-releasing micelle (similar as CORM-3)[13] and RuCO•apo-E45C/C48A-rHLFr (3-fold higher than CORM-3).[10] The non-endocytic uptake of β-PN is beneficial for intracellular delivery with high efficiency compared to specific receptor-mediated endocytosis of RuCO•apo-E45C/C48A-rHLFr.[10,19] Thus, **β-PN_Ru** is an efficient system for delivering high local doses of CO into the intracellular environment because of the high cell-permeability and sustained CO release provided by retention of the $Ru(CO)_2$ moiety on β-PN.

The intracellular CO delivered by **β-PN_Ru** efficiently induces expression of NF-κB target genes by ROS-mediated activation of NF-κB. **β-PN_Ru** induces ROS production within

12 h (Fig. 5a), presumably by binding of the released CO to intracellular heme proteins.[22,45] The ROS-mediated activation of NF-κB results in the expression of the target genes at 12 h (Fig. 4b and 5b). Since continuous activation of NF-κB by excess amounts of ROS causes cell damage,[39,46] it is expected that production of ROS is attenuated at the 24 h time point by the expressed NF-κB target genes such as *HO1* and *NQO1* (Fig. 5a).[25,42,47] The attenuation of ROS production at 24 h inhibited further activation of the target genes (Fig. 5a and 5b). CORM-3 induced *NQO1* expression only at 24 h (Fig. 5b). The effect does not seem to be involved in ROS- and NF-κB-dependent pathway (Fig. 4a and 5a). The opposite trend of **β-PN_Ru** and CORM-3 on *NQO1* expression implies that properties of CO-RMs, such as CO release rate and amount of CO, affect signaling pathways for induction of gene expression. In comparison, TNF-α shows ROS-independent activation of NF-κB, resulting in less of an effect on the expression of the target genes (Fig. 4b and 5). Thus, modulation of amount of ROS by intracellular CO can induce rapid and efficient expression of the NF-κB target genes. It has been reported that CO gas activates NF-κB by generation of ROS, resulting in the expression of the cytoprotective genes under normal physiological conditions.[22,23] However, RuCO•apo-E45C/C48A-rHLFr has no statistically significant effect on NF-κB activity in the absence of TNF-α (Fig. S7), though RuCO•apo-E45C/C48A-rHLFr shows almost comparable $t_{1/2}$ value of CO-release (35.5 min) to **β-PN_Ru** (26.2 min).[10] The comparison suggests that the cellular uptake property of CO-RMs such as uptake mechanism and efficiency is one of the important factors to initiate the signaling pathway involving activation of NF-κB.

Conclusions

In conclusion, the Ru carbonyl-protein needle composite provides efficient intracellular delivery of CO to induce the NF-κB signaling pathway. The protein needle conjugated to $Ru(CO)_2$ moieties retains high cellular permeability and achieves sustained CO release. We demonstrated that CO delivered by **β-PN_Ru** effectively modulates ROS-mediated activation of NF-κB to induce expression of the target genes. It is important to evaluate the intracellular binding sites of CO released from **β-PN_Ru** for further design of CO-releasing protein needles. Development of protein needle-based CO-RMs will provide useful protein-based organometallic tools which will lead to significant advances in elucidation of a number of signaling pathways as well as significant advances in medical applications.

Methods

Construction of protein needle-Ru composites

β-PN_Ru; A methanol solution of CORM-2 (30 μM) was slowly added to an aqueous solution of β-PN (5.0 μM in 20 mM Tris/HCl pH 8.0) and the mixture (final concentration of 20% methanol) was gently stirred at 25°C for 3 h in the dark. **β-PN_Ru** was purified using Sephadex G-25 that was equilibrated with 0.1 M sodium phosphate pH 7.0. The protein recovery after the modification was 26%. UV/Vis: λ_{max} 280 nm (ε ($\mu M^{-1}\cdot cm^{-1}$) = 171300). **β-PN_iRu**; A methanol solution of $Ru(DMSO)_4Cl_2$ (60 μM) was slowly added to an aqueous solution of β-PN (5.0 μM in 20 mM Tris/HCl pH 8.0) and the mixture (final concentration of 20% methanol) was gently stirred at 25°C for 3 h in the dark. **β-PN_iRu** was purified using Sephadex G-25 that was equilibrated with 0.1 M sodium phosphate pH 7.0. The protein recovery after the modification was 25%. UV/Vis: λ_{max} 280 nm (ε ($\mu M^{-1}\cdot cm^{-1}$) = 170200).

Myoglobin (Mb) assay

The assay was carried out according to reported procedure.[8,10] All solutions were degassed by Ar bubbling for 30 min. **β-PN_Ru** (18 μM Ru carbonyl) was added to Mb (6.9 μM) in 10 mM PBS containing 6.9 mM $Na_2S_2O_4$. Absorbance of 250-700 nm was recorded every 1 min for a total of 100 min after the addition of **β-PN_Ru**. Conversion of deoxy-Mb to MbCO was calculated according to the reported procedure.[13] The isosbestic point at 552 nm was adjusted as an internal reference in all spectra. Equivalent of CO per Ru carbonyl and half-life time ($t_{1/2}$) were determined by fitting to pseudo first order kinetics using Excel and Solver (Fig. S3a and S3b).[34]

Oxy-hemoglobin (Oxy-Hb) assay

Bovine blood Hb (Sigma) (20 μM in 10 mM PBS) was reduced with 17.3 mM $Na_2S_2O_4$. The mixture was purified by a desalting column (HiTrap Desalting, GE Healthcare) to obtain oxy-Hb with no residual $Na_2S_2O_4$. **β-PN_Ru** (12 μM Ru carbonyl) was added to the oxy-Hb (5.0 μM). After 90 min incubation, absorbance of 400-700 nm was recorded.

Cellular uptake analysis

The uptake analysis was carried out according to the reported procedure.[13] HEK293/κB-Fluc cells were seeded in a 6-well plate (2.0×10^5 cells/well) and incubated in the presence of **β-PN_Ru** (10 μM Ru carbonyl) or CORM-3 (200 μM Ru carbonyl) in 1 mL medium for 6, 12, or 24 h at 37°C under 5% CO_2. Thereafter the cells were collected by trypsinization and centrifugation. The cells were washed with 1 × PBS and centrifuged again to obtain cell pellets. The pellets were lysed with 50 μL of 10% Tween 20 followed by centrifugation. The concentration of Ru atoms of the cell lysate was determined by ICP-MS. The percentage uptake was calculated from amount of Ru atoms used in the assay and in the cell lysates using a following equation.

$$\text{Uptake (\%)} = \frac{\text{[Ru in cell lysate]} \times \text{Volume of cell lysate}}{\text{[Ru used]} \times \text{Volume of medium}} \times 100$$

where [Ru used] and [Ru in cell lysate] are the concentration of Ru carbonyl used in the assay and Ru atoms in cell lysate, respectively.

Construction of protein needle-ATTO520 composites

ATTO520-modified β-PN: A DMSO solution of ATTO520-maleimide (ATTO-TEC, 90 μM) was added to an aqueous solution of β-PN_G18C (5.0 μM in 20 mM potassium phosphate pH 7.0), and the mixture (final concentration of 5% DMSO) was stirred at 25°C for 15 h in the dark. ATTO520-modified β-PN was purified using Sephadex G-25 that was equilibrated with 0.1 M sodium phosphate pH 7.0. MS (MALDI-TOF): [β-PN_G18C monomer + ATTO520-maleimide]$^+$, calcd.: 15335; found: 15331. ATTO520-modified β-PN_Ru: A methanol solution of CORM-2 (30 μM) was slowly added to an aqueous solution of ATTO520-modified β-PN (5.0 μM in 20 mM Tris/HCl, pH 8.0) and the mixture (final concentration of 20% methanol) was gently stirred at 25°C for 3 h in the dark. ATTO520-modified β-PN_Ru was purified using Sephadex G-25 that was equilibrated with 0.1 M sodium phosphate, pH 7.0.

Cellular uptake of protein needle-ATTO520 composites

HEK293 cells (2.0 × 10^4 cells) were plated onto single-well glass-bottom dishes and cultured in medium at 37°C under 5% CO_2 for 12 h. ATTO520-modified β-PN or ATTO520-modified **β-PN_Ru** (0.83 μM) was added and incubated for 12 h. medium was removed, and the cells were washed with 1 × PBS. The nuclei were labeled with Hoechst 33342 (5 μg/mL) (Invitrogen) by incubating the cells with the dye solution in PBS for 15 min at 37°C under 5% CO_2. The dye solution was removed, and the cells were washed with 1 × PBS. Imaging was performed in fresh cell culture medium. ATTO520-modified samples and Hoechst 33342 were excited with 488 nm and 405 nm and were observed through 525/50 and 450/50 emission filters, respectively.

Intracellular CO Imaging

HEK293/κB-Fluc cells (3.0 × 10^4 cells) were plated onto single-well glass-bottom dishes and cultured in medium at 37°C under 5% CO_2 for 72 h. After removal of the medium, **β-PN_Ru** or CORM-3 (40 μM Ru carbonyl) in fresh medium was added and incubated for 60 min. The medium was removed, and 1 μM COP-1 in phenol red-free medium (Sigma, D5921) was added. The cells were incubated for 30 min at 37°C under 5% CO_2. The cells were excited with 488 nm and observed through 525/50 emission filter. Fluorescence intensity per cell area was measured by ImageJ software from the fluorescence images.[48]

MTT assay

HEK293/κB-Fluc cells (1.0 × 10^4 cells) were seeded in a 96-well plate and incubated with **β-PN_Ru** or CORM-3 in medium for 25 h in at 37°C under 5% CO_2. Thereafter, 10 μL of MTT solution (Sigma, M5655) was added to each well and incubated for 4 h at 37°C under 5% CO_2. After removal of the solution and washing with PBS, 200 μL of DMSO was added. The cells were lysed, and formazan crystals were solubilized by pipetting. Then, the OD at 570 nm was measured using 96-well microplate reader.

NF-κB reporter assay

HEK293/κB-Fluc cells (1.0 × 10^4 cells) were seeded in a 96-well plate. **β-PN_Ru**, **β-PN_iRu**, or CORM-3 (1, 10, or 20 μM Ru) were added to the wells and the cells were cultured for 1 h. TNF-α (0.3 ng/mL) was added to the cells that were pretreated with the buffer (0.1 M sodium phosphate pH 7.0) for 1 h. Then the plates were incubated for 12 or 24 h. At the end of the culture periods, the cells were harvested and lysed with 50 μL lysis buffer. Luciferase activity of cell lysates was measured using the Luciferase Assay Kit (Promega) as described previously.[38]

ROS Measurement

HEK293/κB-Fluc cells (1.0 × 10^4 cells) were cultured in a 96-well plate with 100 μL of medium without phenol red (Sigma, D5921) and incubated for 12 h at 37°C under 5% CO_2. **β-PN_Ru** or CORM-3 were added to each well at 10 μM Ru carbonyl and the cells were cultured for 1 h. TNF-α (1.0 ng/mL) was added to the cells that were pretreated with the buffer (0.1 M sodium phosphate pH 7.0) for 1 h. The cells were incubated for further 6-24 h. Then, the cells were treated with reagents (Promega G8820, ROS-Glo™ H_2O_2 Assay) and luminescence was measured.

Quantitative RT-PCR

HEK293/κB-Fluc cells (2.0 × 10^4 cells) were seeded in 6-well plates. **β-PN_Ru** or CORM-3 were added to each well at 10 μM Ru carbonyl and the cells were cultured for 1 h. TNF-α (1.0 ng/mL) was added to the cells that were pretreated with the buffer (0.1 M sodium phosphate pH 7.0) for 1 h. Then the plates were incubated for 12 or 24 h. Total RNA was extracted from the cells with RNeasy Plus Mini (Qiagen, Valencia, CA, USA) and reversely transcribed using ReverTra Ace-α-^{TM} kit (Toyobo, Tokyo, Japan). Quantitative RT-PCR was carried out with SYBR Thunderbird (Toyobo) using following primers: *Actb* forward 5'-ccaaccgcgagaagatga-3', *Actb* reverse 5'-ccagaggcgtacagggatag-3', *HO1* forward 5'-ggcagagggtgatagaagagg-3', *HO1* reverse 5'-agctcctgcaactcctcaaa-3', *NQO1* forward 5'-atgtatgacaaaggacccttcc-3', *NQO1* reverse 5'-tcccttgcagagagtacatgg-3', *IL6* forward 5'-caggagcccagctatgaact-3', *IL6* reverse 5'-gaaggcagcaggcaacac-3'.

Statistical analysis

Statistical analyses included the Student's t test. Values of $P < 0.05$ were considered statistically significant.

Acknowledgements

We thank CeMI for assistance with confocal microscopy. This work was supported by a Research Fellowship for Young Scientists of JSPS for H.I. (No. 4240) and Fundings are from Next-Generation World-Leading Researchers (No. LR019) from Ministry of Education, Culture, Sports, Science and

Technology, JSPS Grant-in-Aid for Scientific Research on Innovative Areas "Dynamical ordering of biomolecular systems for creation of integrated functions" (No. 26102513), "Molecular Robotics" (No.15H00805), for challenging Exploratory Research (No. 26560433), and from a Sekisui Chemical Grant Program for Research, Sekisui Nature-Tech Foundation Program, Mitsubishi Foundation, Japan. iCeMS is supported by the World Premier International Research Initiative (WPI), MEXT, Japan.

Notes and references

1 C. C. Romão, W. A. Blättler, J. D. Seixas and G. J. L. Bernardes, *Chem. Soc. Rev.*, 2012, **41**, 3571–3583.
2 R. Motterlini and L. E. Otterbein, *Nat. Rev. Drug Discov.*, 2010, **9**, 728–743.
3 L. E. Otterbein, F. H. Bach, J. Alam, M. Soares, H. Tao Lu, M. Wysk, R. J. Davis, R. A. Flavell and A. M. Choi, *Nat. Med.*, 2000, **6**, 422–428.
4 C. A. Piantadosi, *Free Radic. Biol. Med.*, 2008, **45**, 562–569.
5 S. García-Gallego and G. J. L. Bernardes, *Angew. Chem. Int. Ed.*, 2014, **53**, 9712–9721.
6 B. E. Mann, *Organometallics*, 2012, **31**, 5728–5735.
7 T. R. Johnson, B. E. Mann, J. E. Clark, R. Foresti, C. J. Green and R. Motterlini, *Angew. Chem. Int. Ed.*, 2003, **42**, 3722–3729.
8 R. Motterlini, J. E. Clark, R. Foresti, P. Sarathchandra, B. E. Mann and C. J. Green, *Circ. Res.*, 2002, **90**, e17–e24.
9 J. E. Clark, P. Naughton, S. Shurey, C. J. Green, T. R. Johnson, B. E. Mann, R. Foresti and R. Motterlini, *Circ. Res.*, 2003, **93**, e2–e8.
10 K. Fujita, Y. Tanaka, T. Sho, S. Ozeki, S. Abe, T. Hikage, T. Kuchimaru, S. Kizaka-Kondoh and T. Ueno, *J. Am. Chem. Soc.*, 2014, **136**, 16902–16908.
11 T. Santos-Silva, A. Mukhopadhyay, J. D. Seixas, G. J. L. Bernardes, C. C. Romão and M. J. Romão, *J. Am. Chem. Soc.*, 2011, **133**, 1192–1195.
12 H. Tabe, K. Fujita, S. Abe, M. Tsujimoto, T. Kuchimaru, S. Kizaka-Kondoh, M. Takano, S. Kitagawa and T. Ueno, *Inorg. Chem.*, 2015, **54**, 215–220.
13 U. Hasegawa, A. J. van der Vlies, E. Simeoni, C. Wandrey and J. A. Hubbell, *J. Am. Chem. Soc.*, 2010, **132**, 18273–18280.
14 G. Dördelmann, H. Pfeiffer, A. Birkner and U. Schatzschneider, *Inorg. Chem.*, 2011, **50**, 4362–4367.
15 G. Dördelmann, T. Meinhardt, T. Sowik, A. Krueger and U. Schatzschneider, *Chem. Commun.*, 2012, **48**, 11528–11530.
16 N. E. Brueckmann, M. Wahl, G. J. Reiß, M. Kohns, W. Waetjen and P. C. Kunz, *Eur. J. Inorg. Chem.*, 2011, 4571–4577.
17 P. Govender, S. Pai, U. Schatzschneider and G. S. Smith, *Inorg. Chem.*, 2013, **52**, 5470–5478.
18 N. Yokoi, H. Inaba, M. Terauchi, A. Z. Stieg, N. J. M. Sanghamitra, T. Koshiyama, K. Yutani, S. Kanamaru, F. Arisaka, T. Hikage, A. Suzuki, T. Yamane, J. K. Gimzewski, Y. Watanabe, S. Kitagawa and T. Ueno, *Small*, 2010, **6**, 1873–1879.
19 N. J. M. Sanghamitra, H. Inaba, F. Arisaka, D. O. Wang, S. Kanamaru, S. Kitagawa and T. Ueno, *Mol BioSyst*, 2014, **10**, 2677–2683.
20 H. Inaba, N. J. M. Sanghamitra, T. Fukai, T. Matsumoto, K. Nishijo, S. Kanamaru, F. Arisaka, S. Kitagawa and T. Ueno, *Chem. Lett.*, 2014, **43**, 1505–1507.
21 M. P. Soares, A. Usheva, S. Brouard, P. O. Berberat, L. Gunther, E. Tobiasch and F. H. Bach, *Antioxid. Redox Signal.*, 2002, **4**, 321–329.
22 H. S. Kim, P. A. Loughran, J. Rao, T. R. Billiar and B. S. Zuckerbraun, *Am. J. Physiol. Gastrointest. Liver Physiol.*, 2008, **295**, G146–G152.
23 B. S. Zuckerbraun, T. R. Billiar, S. L. Otterbein, P. K. M. Kim, F. Liu, A. M. K. Choi, F. H. Bach and L. E. Otterbein, *J. Exp. Med.*, 2003, **198**, 1707–1716.
24 K. Maruyama, E. Morishita, T. Yuno, A. Sekiya, H. Asakura, S. Ohtake and A. Yachie, *Thromb. Res.*, 2012, **130**, e188–e193.
25 P.-L. Chi, C.-J. Liu, I.-T. Lee, Y.-W. Chen, L.-D. Hsiao and C.-M. Yang, *Mediators Inflamm.*, 2014, **2014**, 1–18.
26 H. Song, C. Bergstrasser, N. Rafat, S. Höger, M. Schmidt, N. Endres, M. Goebeler, J. L. Hillebrands, R. Brigelius-Flohé, A. Banning, G. Beck, R. Loesel and B. A. Yard, *Br. J. Pharmacol.*, 2009, **157**, 769–780.
27 T. Takagi, Y. Naito, K. Uchiyama, T. Suzuki, I. Hirata, K. Mizushima, H. Tsuboi, N. Hayashi, O. Handa, T. Ishikawa, N. Yagi, S. Kokura, H. Ichikawa and T. Yoshikawa, *Dig. Dis. Sci.*, 2011, **56**, 1663–1671.
28 B. Sun, X. Zou, Y. Chen, P. Zhang and G. Shi, *Int. J. Biol. Sci.*, 2008, **4**, 270–278.
29 G. Cepinskas, K. Katada, A. Bihari and R. F. Potter, *Am. J. Physiol. Gastrointest. Liver Physiol.*, 2008, **294**, G184–G191.
30 H. Song, H. Zhao, Y. Qu, Q. Sun, F. Zhang, Z. Du, W. Liang, Y. Qi and P. Yang, *J. Periodontal Res.*, 2011, **46**, 48–57.
31 J. Megías, J. Busserolles and M. J. Alcaraz, *Br. J. Pharmacol.*, 2007, **150**, 977–986.
32 S. Knecht, D. Ricklin, A. N. Eberle and B. Ernst, *J. Mol. Recognit.*, 2009, **22**, 270–279.
33 M. J. Cleare and W. P. Griffith, *J. Chem. Soc., A*, 1969, 372–380.
34 L. Hewison, S. H. Crook, B. E. Mann, A. J. H. M. Meijer, H. Adams, P. Sawle and R. A. Motterlini, *Organometallics*, 2012, **31**, 5823–5834.
35 S. McLean, B. E. Mann and R. K. Poole, *Anal. Biochem.*, 2012, **427**, 36–40.
36 G. Saito, J. A. Swanson and K. D. Lee, *Adv. Drug Deliv. Rev.*, 2003, **55**, 199–215.
37 B. W. Michel, A. R. Lippert and C. J. Chang, *J. Am. Chem. Soc.*, 2012, **134**, 15668–15671.
38 L. Zeng, S. Kizaka-Kondoh, S. Itasaka, X. Xie, M. Inoue, K. Tanimoto, K. Shibuya and M. Hiraoka, *Cancer Sci.*, 2007, **98**, 1394–1401.
39 M. Bilban, A. Haschemi, B. Wegiel, B. Y. Chin, O. Wagner and L. E. Otterbein, *J. Mol. Med.*, 2008, **86**, 267–279.
40 N. G. Abraham and A. Kappas, *Pharmacol. Rev.*, 2008, **60**, 79–127.
41 P. Tsvetkov, N. Reuven and Y. Shaul, *Cell Death Differ.*, 2010, **17**, 103–108.
42 H. J. Kim, M. Zheng, S.-K. Kim, J. J. Cho, C. H. Shin, Y. Joe and H. T. Chung, *Immune Netw.*, 2011, **11**, 376–382.
43 K. S. Ahn, G. Sethi, A. K. Jain, A. K. Jaiswal and B. B. Aggarwal, *J. Biol. Chem.*, 2006, **281**, 19798–19808.
44 K. Miyazawa, A. Mori, K. Yamamoto and H. Okudaira, *Am. J. Pathol.*, 1998, **152**, 793–803.
45 C. Taillé, J. El-Benna, S. Lanone, J. Boczkowski and R. Motterlini, *J. Biol. Chem.*, 2005, **280**, 25350–25360.
46 S. Nakajima and M. Kitamura, *Free Radic. Biol. Med.*, 2013, **65**, 162–174.
47 M. J. Morgan and Z.-G. Liu, *Cell Res.*, 2011, **21**, 103–115.
48 O. Gavet and J. Pines, *Dev. Cell*, 2010, **18**, 533–543.